Nucleobase catalysts for the enzymatic activation of 8-oxoguanine DNA glycosylase 1

Emily C. Hank,[1, #] Nicholas D'Arcy-Evans,[1] Emma Rose Scaletti,[2] Carlos Benítez-Buelga,[3, 4] Olov Wallner,[1] Florian Ortis,[1] Kaixin Zhou,[1] Liuzhen Meng,[1] Patricia Calvo,[5] Ingrid Almlöf,[1] Elisée Wiita,[1] Sara Košenina,[2] Andreas Krämer,[6] Maeve Long,[1] Ann-Sofie Jemth,[1] Holly Dawson,[1] Josephine Stewart,[1] Adam Dickey,[1] Mikhael E. Astorga,[1] Marek Varga,[1] Evert J. Homan,[1] Martin Scobie,[1] Stefan Knapp,[6] Miguel de Vega,[5] Leandro Sastre,[3, 7] Pål Stenmark,[2, 8] Thomas Helleday,[1, 9] Maurice Michel[1, *]

AUTHOR ADDRESS

1 Science for Life Laboratory, Department of Oncology-Pathology, Karolinska Institutet, Stockholm, Sweden

2 Department of Biochemistry and Biophysics, Stockholm University, Stockholm, Sweden

3 Instituto de Investigaciones Biomédicas Alberto Sols CSIC/UAM, Madrid, Spain

4 Molecular Genetics Unit, Instituto de Investigación de Enfermedades Raras (IIER), Instituto de Salud Carlos III (ISCIII), Madrid, Spain.

5 Centro de Biología Molecular 'Severo Ochoa' (CSIC-UAM), Madrid, Spain

6 Institute of Pharmaceutical Chemistry & Structural Genomics Consortium (SGC), Goethe University, Frankfurt, Germany

7 Centro de Investigación Biomédica en Red de Enfermedades Raras (CIBERER). Instituto de Salud Carlos III. C., Madrid, Spain

8 Department of Experimental Medical Science, Lund University, Lund, Sweden

9 Weston Park Cancer Centre and Division of Clinical Medicine, School of Medicine and Population Health, University of Sheffield, Sheffield, United Kingdom

Current Address: Department of Pharmacy, Ludwig-Maximilians-Universität Munich, Germany

KEYWORDS: Base excision repair, OGG1, organocatalytic switch, DNA glycosylase, thioguanine

Graphical abstract: OGG1 activators acting from within the catalytic pocket are organocatalytic switches that enhance DNA repair through stimulating rudimentary activities or establishing de novo enzymatic functions on a widened substrate scope.

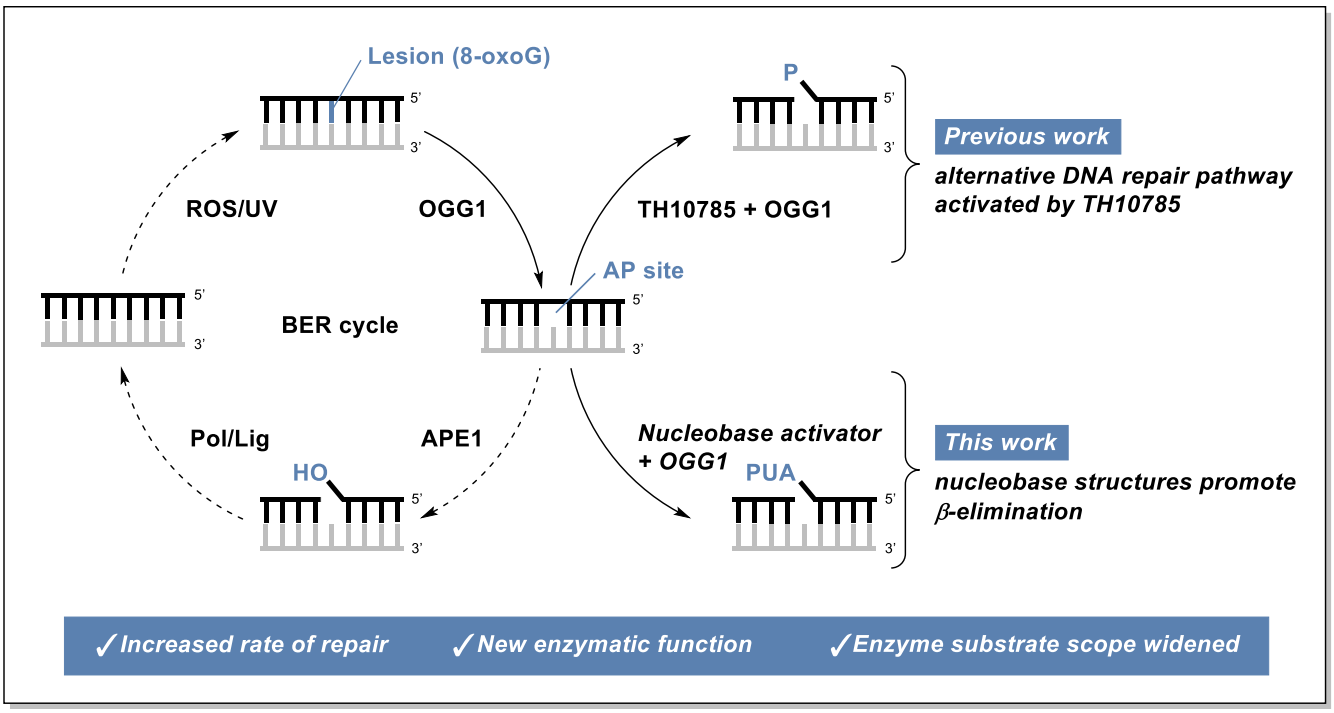

ABSTRACT: Bifunctional DNA glycosylases employ an active site lysine or the N-terminus to form a Schiff base with the abasic site (AP site) base excision repair (BER) intermediate. Cleaving this reversible structure is the rate-determining step in the initiation of 8-oxoguanine (8-oxoG) repair for 8-oxoguanine DNA glycosylase 1 (OGG1). The OGG1 AP lyase activity can be increased using small molecule binders, called organocatalytic switches, to cleave the DNA backbone in a similar

manner as a bifunctional DNA glycosylase. In search for novel organocatalytic switches we here identify 8-Substituted 6-thioguanines and 6-amino-pyrazolo-[3,4-*d*]-pyrimidine derivatives as potent and selective scaffolds enabling OGG1 to cleave AP sites opposite any canonical nucleobase by β-elimination, shaping a complete, artificial AP-lyase function. These new tool compounds enhance the cellular repair of 8-oxoG and AP sites, activating a rudimentary but canonical enzymatic activity.

Oxidative damage in the form of 8-oxoG is the most common DNA lesion in our cells. An accumulation of 8-oxoG, its oxidation products or subsequent mutations caused through their presence leads to deterioration of cellular health and ultimately to neurodegenerative[1,2] and cardiovascular [3,4] diseases, as well as cancer.[5,6] OGG1 is the enzyme responsible for the removal of 8-oxoG and the literature suggests that targeting of OGG1 function may be a viable strategy to counter-act these effects.[7,8] In addition to an allosteric mechanism,[9] pharmacological OGG1 activation has been reported to act by enhancing an otherwise rudimentary AP-lyase activity.[10] This AP-lyase activity is most likely controlled by product-assisted catalysis; a distinct mode of action compared to classic allosteric regulation.[11] Here, 8-oxoG acts as a weak chemical base and abstracts a proton from the Schiff base intermediate formed between the AP site and OGG1 active site Lys249. *In vitro*, this process results in a weak AP-lyase activity through *β*-elimination, which leads to 3'-DNA strand incision and removal of OGG1 from the product. In cells, this effect is negligible and OGG1 is thus a monofunctional glycosylase. OGG1 is only released from the Schiff base intermediate through the function of recruited apurinic/apyrimidinic endonuclease 1 (APE1),[12] rendering it the rate-determining step in the initiation of BER.

In agreement with the product-assisted catalysis mechanism postulated by Fromme *et al.,*[11] we have recently reported OGG1 activators, also called organocatalytic switches, of an artificial *β,δ*-elimination, releasing a 5'-incised DNA product. These compounds comprise a two-component system, containing a heterocyclic nitrogen center with Brönsted base-like character and a structural handle with active site affinity. Furthermore, we used 8-bromoguanine as a more soluble analogue of 8-oxoG and confirmed it to be an activator of *β*-elimination (Figure 1). To investigate the mechanism of this *β*-elimination in detail and the chemical space surrounding purine-based organocatalytic switches of OGG1, we started by screening a 500 compound in-house library of nucleobase analogues. Using our in-house fluorescence-based assay, we measured the concentration of half maximal activation (AC_{50})[10] to quantify the enhancement of OGG1 mediated DNA incision. We counter-screened all active compounds for DNA intercalation, auto-fluorescence and APE1 interaction. Among the primary hits were the FDA approved drugs thioguanine **1** and azathioprine **2** (Figure 1, Figure S1), 8-substituted thioguanines **3-5** and compounds combining guanine with amines in the 6-position (**6-9**).

Based on these screening results, we initially directed our attention towards the hits within the 6-thioguanine series. We generated a number of analogues of 8-substituted 6-thioguanines with larger substituents (Table 1, Table S1A). Interestingly, only small substituents were tolerated in the 8-position, as observed for compounds **3** and **10**. We then explored the apparent necessity of an unsubstituted 6-thio modification by generating analogues with thioether or sulfone modifications (Table S1B). Again, small substituents gave better results, while extended systems were inactive below 100 μM. A combination of small substituents in both the 6-thioether as well as the 8-position failed to further improve the activity of thioguanine based organocatalytic switches of OGG1. These studies suggest a highly specific structure activity relationship (SAR) for thioguanines, allowing only minor modifications to the core system.

To follow up on the primary hits with a 6-amino substituted guanine core (Table 1, Table S2), we generated analogues using different amines. With the exception of the 3,4-dichloro analogue **11** (Figure S2), aniline substitution did not lead to improved compound properties. Further, we generated matched pair compounds for the thioguanines synthesized previously. Given active site binding, this comparison suggested that guanines require a secondary amine, namely an R_1R_2–NH, between the two parts of the molecule to be able to activate OGG1. This informed the requirement for H-bonding in addition to π-stacking with the bicyclic hetero-aryl system. Having established the 3,4-dichloroaniline substituent, we then investigated the scope of accepted nucleobase analogues and purine scaffolds, replacing guanine with adenine, uracil and other heterocycles (Table S3A). A 6-amino-pyrazolo-[3,4-*d*]-pyrimidine derivative **12** surpassed guanine analogue **11** in the biochemical assay (Table 1). Following this finding, we assembled a number of matched pairs based on previously synthesized 6-aminoaryl-guanines (Table S3B) and observed that all members of the pyrazolo-[3,4-*d*]-pyrimidine series surpassed the activity of their guanine counterparts. These results suggest that a series of OGG1 organocatalytic switches derived from nucleobases may be

informed by previously observed OGG1 inhibitor chemical space to optimize the affinity handle of the molecules.[13] At the same time, the polar and nitrogen-rich scaffold of nucleobases appears suitable to stimulate proton abstraction during OGG1 catalysis.

Figure 1: Screening for OGG1 organocatalytic switches based on substrate similarity: A number of OGG1 organocatalytic switches have previously been reported. As an 8-oxoG analogue, 8-bromoguanine is a known OGG1 activator catalyzing the inherent β-elimination activity of OGG1. Based on substrate similarity we screened an in-house library of diverse modified nucleobases and discovered 8-methylpurines as potent OGG1 organocatalytic switches (**3**-**5**). Additional classes covered thioguanine analogues including FDA-approved drugs (**1**, **2**), as well as 6-amino-substituted guanines (**6**-**9**) but not adenines or 9-substituted nucleobases. Assay Details in Methods and Material.

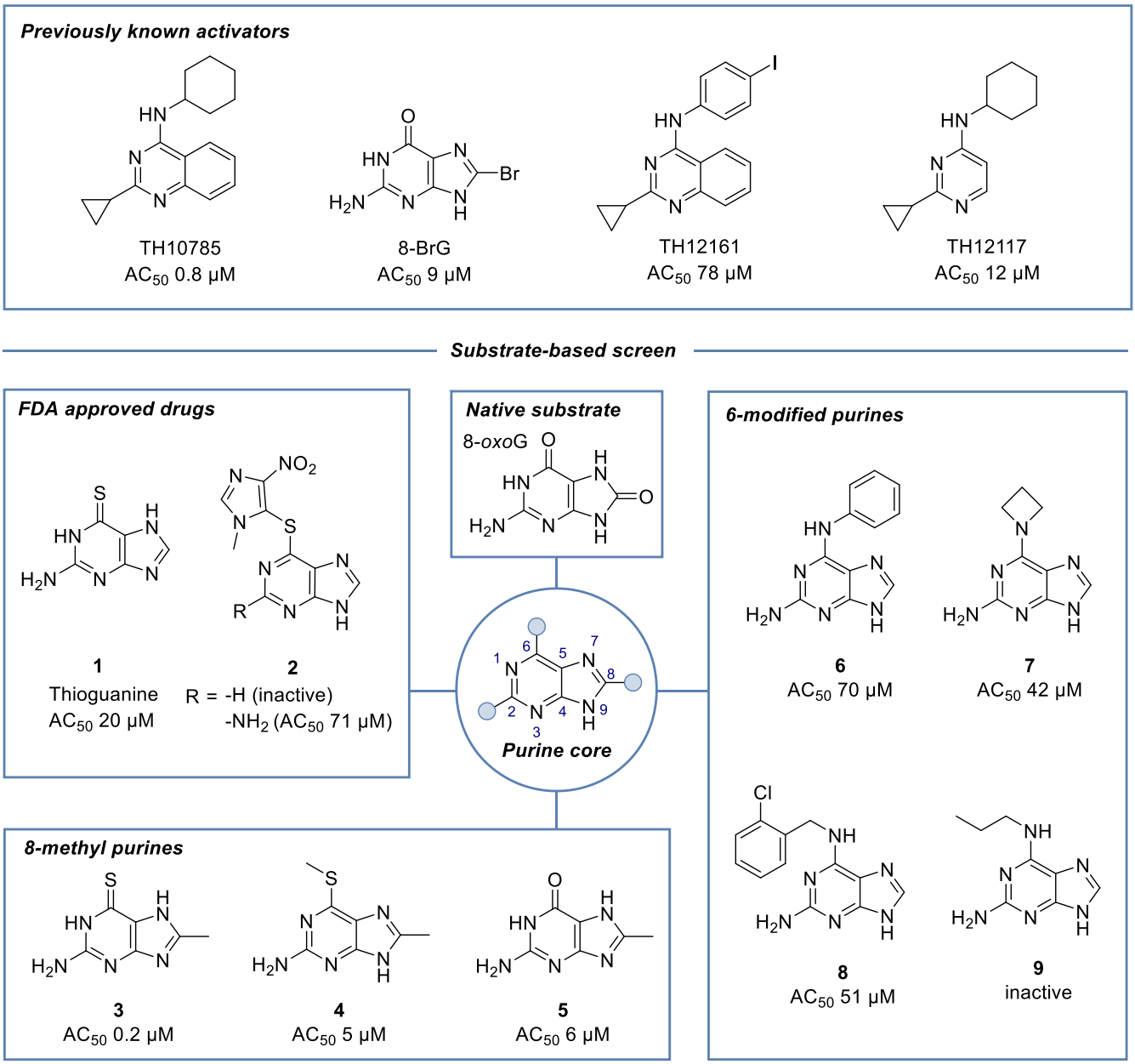

Table 1: Optimization towards potent and selective OGG1 organocatalytic switches: Assay Details in Methods and Material. AC_{50} in µM, CI95 confidence interval 95% in µM; * compound only reaches AC_{35} due to a bell-shape activity curve.

#	structure	AC_{50} (CI 95) [µM]
3	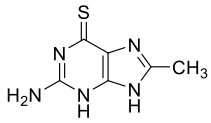	0.32 (0.27 - 0.39)
10	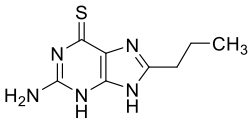	0.55 (0.26 - 1.20)
11	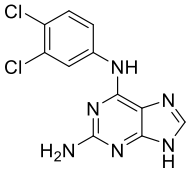	12.5*
12	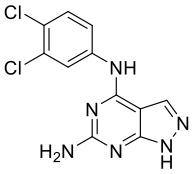	13.1 (2.3-75.1)
13	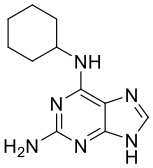	>100
14	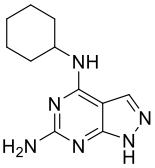	11.7 (5.5-24.9)
15	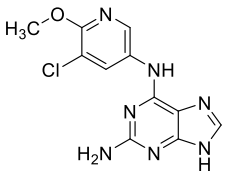	28.2 (10.0-79.8)

We then elucidated the exact nature of the observed OGG1 biochemical activity using a ^{32}P-radiolabelled substrate and resolution by PAGE (Figure 2A, Figure S3). Compounds **13** and **3** as members of their respective nucleobase series were confirmed as activators of the inherent β-lyase activity. In short time frames, the phosphatase activity of T4PNK[14] had no effect on the 3'-phospho unsaturated aldehyde product generated through **13** and **3**, as opposed to TH10785 which generated a 5'-phosphate product as substrate for T4PNK. Longer incubation with **13** and **3** also generated minor amounts of the 5'-phosphate product (Figure S3).

Due to the need to utilize a nucleophilic lysine residue and cleavage of a Schiff base *via* proton abstraction, OGG1 functions optimally at a pH close to 8.[10] We previously observed a pH optimum of 7.5 for activity of TH10785 and thus performed all AC_{50} measurements during screening and optimization at a pH of 7.5. Given this dynamic interplay between OGG1 modulator and enzyme, we then assessed the artificially controlled AP-lyase activity across a range of pH values. We measured the initial rate of the reaction using the 8-oxoA substrate and compounds **3**, TH10785 and **14** (Figure 2B). Choosing the most potent concentrations of each compound, we observed that all compounds showed a tendency to activate OGG1 at a pH closer to their individual pKa (TH10785 (1N: 6.55 ± 1.13), **3** (9N: 2.59 ± 2.22) and **14** (9N, 13.53 ± 2.00)). These findings confirmed the crucial role of a basic nitrogen. Investigating the effects on the entire system, we assessed protein stability using the melting temperature at different pH and in the presence of the compounds using Nano-DSF (Table S4). The presence of the employed compounds led to a general increase in protein stability, as well as an increase in stability at extreme pH similar to compound pKa, which may partly explain the observed enhancement of enzymatic activity in the biochemical assay through binding of the compounds to OGG1. Using D_2O as solvent, we further investigated a solvent isotope effect within the in-house fluorescence-based assay and observed challenged incision efficacy evidenced by the slower rate of the reaction compared to conditions using H_2O (Figure S4). Altogether, these investigations draw a complex picture of protein stability, compound binding, proton abstraction and transfer, as well as substrate and leaving group solvation during elimination events.

Since OGG1 has a preference for 8-oxoG opposite cytosine,[15] we hypothesized that a substantially increased AP-lyase function could overwrite this cytosine selectivity. Thus, we performed saturation kinetics with OGG1 against the substrates 8-oxoA:C and AP:A, AP:C, AP:G and AP:T, generated from their respective uracil containing precursors using UNG2. Using **3** and TH10785 to evaluate a potential influence of *β*- or *β,δ*-elimination capabilities, we found that both compounds pronounced the inherent preference for cytosine (Figure 2C, Figure S5). Further, both compounds exhibited a strong saturation effect for the 8-oxoA substrate that surpassed those observed for the AP-site substrates. This indicated competition through active site binding.[10] In contrast to TH10785, **3** was able to stimulate a significant OGG1 AP-lyase function on all substrates, suggesting that compound potency and not the type of AP-lyase function governs the reaction on AP-sites.

To confirm active site binding we evaluated the biochemical activity of **3** and **14** on OGG1 mutant variants. While incision through wtOGG1 and Ser326Cys were enhanced, active site mutants Phe319Ala, Cys253Tyr and Lys249Trp were not affected by incubation with the compounds, suggesting that the activity of the compounds is exerted from within the active site (Figure 2D). This finding was corroborated by solving the X-ray co-crystal structures of mouse OGG1 in complex with **3**, **10**, **14** and **15** confirming active site binding (Figure 2E-H, Figure S6). The binding poses of compounds **14** and **15**, interacting both with Phe319 and Gly42, confirmed the selectivity observed within the structure activity relationship. An overlay with the 8-oxoG-bound human OGG1 (PDB ID: 1HU0)[11] indicated no significant rearrangements in the core protein structure for all structures solved. Identical placement of **3**, **10** and 8-oxoG (Figure 2G-H, Figure S7) suggests a binding mode that allows for enhanced product-assisted catalysis. The heterocyclic ring systems of **14** and **15** are observed to be shifted outwards due to their more spacious 6-amino substitution and are also flipped compared to one another, which may explain the lower activity observed for this series in all assays (Figure S7).

To rule out any unwanted effects of the molecules regarding potential toxicity or off-target effects, we extensively profiled TH10785, **3** and **14** using an in-house functional panel of enzymes consisting of DNA glycosylases,[16] NUDIX family members[17,18] and a set of protein kinases probed using thermal stability.[19] All tests returned negative for off-targets (Table S6-7). Cultivation of an immortalized cell line, BJ-TERT, and an oncogene driven cell line, BJ-Ras,[20,21] over several days in the presence of a dose response of the compounds confirmed the absence of any toxicity between these two cell lines (Table S8).

Using the selective and non-cytotoxic scaffolds **10** and **14**, we investigated whether OGG1 function was indeed improved in a cellular setting. We induced DNA damage using $KBrO_3$ and profiled both 8-oxoG and AP sites. As before, we observed increased levels of nuclear 8-oxoG over 6 hours post exposure (Figure 2I). This effect was rescued by OGG1 organocatalytic switches. The cellular efficacy thereby followed the biochemical activity for organocatalytic switches of the β-elimination, as **10** was superior to **14**, with TH10785 being most efficient. This indeed indicated an increased cellular repair of 8-oxoG lesions in DNA. However, considering that the compounds

redirect OGG1 function towards resolving AP sites, we expected a more pronounced effect for analogues **10** and **14** when assessing the levels of this particular type of DNA damage. Using the aldehyde reactive probe[22] and fluorescence-activated cell sorting we observed reduced numbers of AP sites for compound **10**, performing at the level of TH10785 (Figure 2J). **14** was found to be inactive at these concentrations, indicating inactivity on the OGG1 enzyme. Collectively, these studies confirm enhanced, compound-mediated OGG1 activity in repairing oxidative DNA damage *in vitro* and in cells.

We here present our efforts in profiling the nucleobase chemical space for organocatalytic switches of the enzyme OGG1 and discover two distinct selective chemical series. These molecules activate the canonical but rudimentary *β*-elimination activity of OGG1 from within the active site of the protein. Active site affinity and a reactive center in the form of a basic nitrogen are combined in one molecule, as evidenced by studies involving OGG1 mutants, substrate scope, generated products and enzymatic activity covering a range of pH environments. Co-crystal structures of a number of analogues further confirm the product-assisted hypothesis of Fromme *et al.* and paint a detailed picture of functional enhancement of enzymatic activity on Schiff bases.

In conclusion, we demonstrate that a chemical space beyond TH10785 exists, that increases the repair of OGG1. Importantly, we here show that these OGG1 organocatalytic switches may act through a distinct mechanism of action and in contrast to TH10785 primarily stimulate the β-elimination during OGG1 catalysis. OGG1 modulators that enhance enzymatic activity are the first chemical entities that rewrite an enzymatic function in cells, allowing for increased DNA damage repair. Considering the widespread implications of OGG1 function within a number of diseases, including neurodegeneration,[1,2] obesity[3,4] and inflammation,[7,23] these small molecules are novel, powerful tools to unravel disease biology, and offer the potential for further development into promising drug candidates.

Figure 2: Nucleobase inspired organocatalytic switches stimulate DNA repair by OGG1: A) Effect of the compounds on the AP-lyase activity of *h*OGG1 on 8oxoG:C-containing DNA. The assay was performed as described in Materials and Methods using 2 nM of the indicated [^{32}P]5'-labeled 8-oxoG-containing substrate, in the presence of 10 nM *h*OGG1, 20 mM EDTA and either 10% DMSO or 6.25 μM for TH10785, **13** and **3**; 50 μM for TH5487 reflecting the best concentrations from the corresponding fluorescence based biochemical assay. After incubation for the indicated times at 37°C, reactions were either stopped or further incubated 10 min in the presence of T4 PNK (+). After incubation samples were analyzed by 7M urea-20% PAGE and autoradiography. Position of products is indicated. Longer incubation shown in Supporting Information. **B)** Compound pKa governs pH range of enzymatic activity: left: **3** activates OGG1 at a pH closer to 7 and below; middle: TH10785 follows a bell-shaped curve with a maximum at pH 7.5; right: **14** has a high pKa and thus controls OGG1 function at a pH above 8. 10 nM 8-oxo:A was used as substrate and was incubated with 10 nM hOGG1. Compounds were used at most effective concentation as indicated and v_0 was measured within the initial linear slope of the reaction. **C)** Saturation kinetics for TH10785 and **3** against a number of AP site substrates and 8-oxoA:C. left: TH10785 activates OGG1 on AP sites opposite any canonical nucleobase; right: **3** follows a similar pattern and all AP sites are more efficiently addressed than 8-oxo substrates. v_0 of reaction was measured. 10 nM 8-oxo:A was used as substrate and was incubated with 10 nM hOGG1. U:X substrate was used to gnerate AP sites opposite canoncial nucleobases using 1 nM UNG2. v_0 was measured within the initial linear slope of the reaction. Details in Materials and Methods. **D)** Assessment of OGG1 mutants confirms activation of variants with changes outside but not within the active site: left: **3** and right: **14** are enhancing wtOGG1 and the S326C mutant, but not F319A, C253Y and K249W. 10 nM 8-oxo:A was used as substrate and was incubated with 10 nM hOGG1. Compounds were assayed with the respective mutants and the initial slope was measured. Assay details in Materials and Methods; **E)** Superposition of mOGG1-**15** (green) and mOGG1-**14** (blue) and hOGG1-DNA-8oxoG (magenta, PDB ID: 1HU0) monomers. DNA from the 8oxoG complex is coloured light orange. Ligands are depicted as sticks; C atoms are coloured green (**15**), blue (**14**) or magenta (8-oxoG), O atoms red, and N atoms dark blue; **F)** Comparison of ligand binding between the structures. Amino acids which contribute to ligand positioning are depicted as thin sticks; **G)** Superposition of mOGG1-**3** (green) and mOGG1-**10** (blue) and hOGG1-DNA-8-oxoG (magenta, PDB ID: 1HU0) monomers. DNA from the 8oxoG complex is coloured light orange. Ligands are depicted as sticks; C atoms are coloured green (**3**), blue (**10**) or magenta (8-oxoG), O atoms red, N atoms dark blue and S atoms gold; **H)** Comparison of ligand binding between the structures. Amino acids which contribute to ligand positioning are depicted as thin sticks; **I)** Effect of activators (TH10785, **14** and **10**) in cells. Quantification of nuclear 8-oxoG levels across different time points in U2OS cells exposed to organocatalytic switches or DMSO, under oxidative stress conditions (20mM of $KBrO_3$ for 1h). Each bar represents the mean ± SEM. Data are the average of three independent experiments. For each experiment, 25 fields and around 1000 cells were captured per condition. Statistical significance was calculated using two-way ANOVA for multiple comparisons. ns, non-significant; *P < 0.05; ****P < 0.0001; **J)** A comparative analysis of ARP-STREP_PE signal induction over DMSO, reported in percentage, is shown. Each

bar represents the mean ± SD. Data are the average of five independent experiments with at least three biological replicates each. Statistical significance was calculated using an unpaired two-tailed Student's t-test. ns, non-significant; ***P < 0.001; ****P < 0.0001.

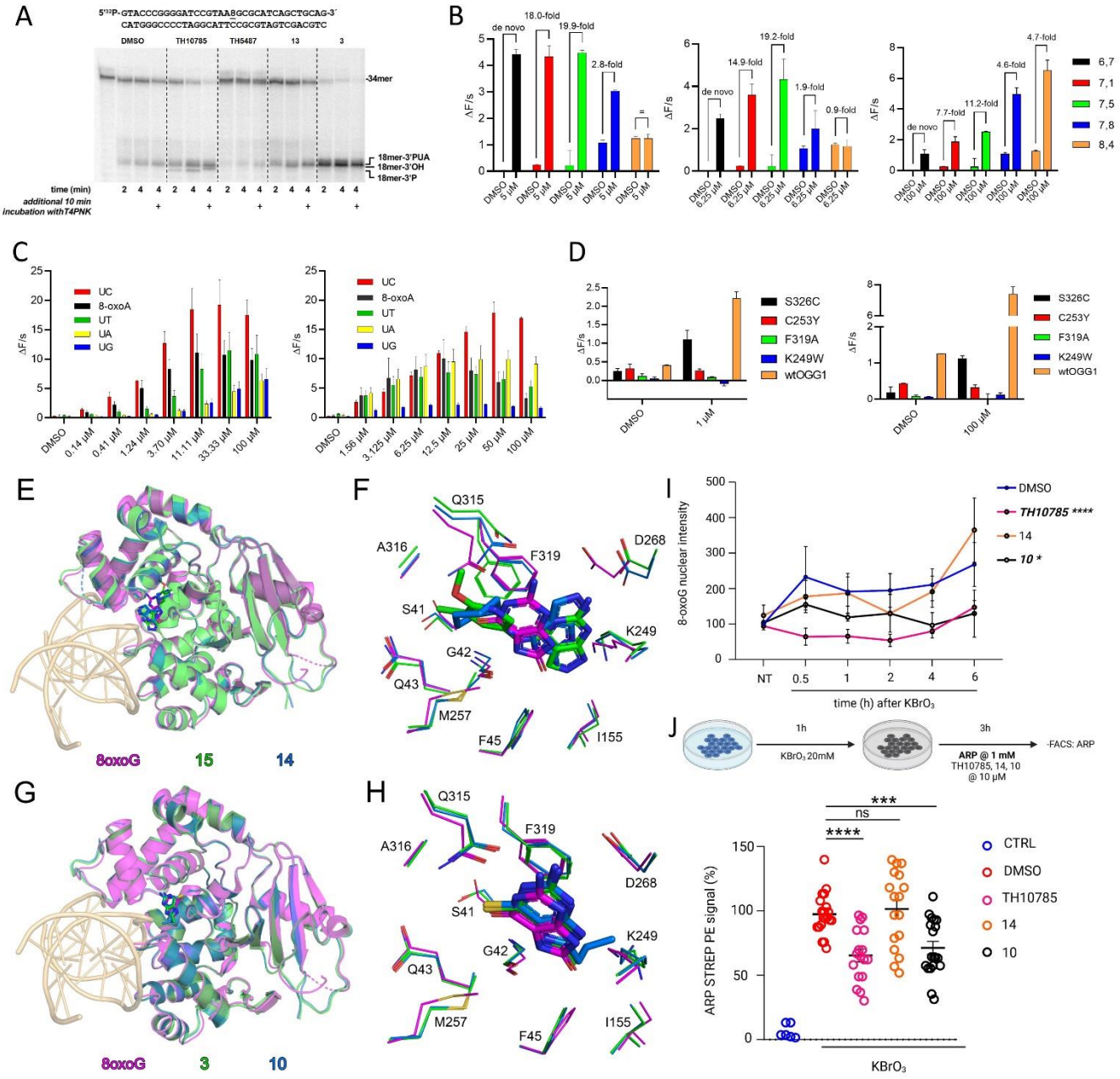

AUTHOR INFORMATION

Corresponding Author

* Maurice Michel: maurice.michel@ki.se

Science for Life Laboratory, Department of Oncology and Pathology, Karolinska Institutet

Author Contributions

Chemical synthesis: ECH, NDE, OW, FO, AD, MEA, JS and MM. Biochemistry: ECH, NDE, LM, PC, KZ, EW, AK, HD, ASJ, MdV and MM. Structural Biology: ERS, SK and PS. Computational Chemistry: EJH, NDE and MM. Cell Biology: CBB, IA, ML and MM. Supervision: OW, ASJ, MS, PS, MdV, SKn, LS, TH and MM. Funding: TH, PS, MdV, CBB, LS, SKn and MM. Writing and Editing: ECH, NDE, OW and MM. Conceptualization: ECH, NDE and MM.

ACKNOWLEDGMENTS

We would like to thank the Chemical Biology Consortium Sweden (CBCS), the Drug Discovery and Development Platform (DDDP), the Protein science facility (PSF) at Karolinska and the Structural Genomics Consortium (SGC) at Karolinska and Goethe-Universität Frankfurt for support. We are thankful to Athina Pliakou, Mari Kullman Magnusson, Kristina Edfeldt, Therese Pham, Mario Kehler and Michael Sundström for administrative support. We thank MAXIV Laboratory (Sweden, proposal MX20200204), Diamond Light Source (United Kingdom, proposals MX15806 and MX21625), and their scientists from the BioMAX and I03 beamlines for their support during data collection.

FUNDING

This work was funded by the European Research Council (TAROX Programme), the Swedish Research Council (2018–03406 PS, 2015-00162 TH), the Alfred Österlund foundation (PS), the Crafoord foundation (20190532 PS), the Helleday Foundation (FO, LM), the Swedish Cancer Society (CAN2021/1490 TH, CAN 2017/716 PS), the Åke-Olsson foundation for haematological research (2020-00306 MM), a Novo Nordisk Pioneer Innovator Grant (NNF23OC0085944 MM), Karolinska Institutet Research Foundation Grants (2020-02186 and 2022-01776 MM), a Childhood Cancer Research Postdoctoral grant (ML), the Åke Wiberg Foundation (M23-0043 MM), Grant PID2020-115978GB-I00 (MdV) funded by MCIN/AEI/10.13039/501100011033, a Health Research Fund, Carlos III Health Institute, co-funded by European Regional Development (FEDER) funds (PI20-00335 LSG) and the Research Talent Attraction Grants (2023-T1/SAL-GL-29292 CBB). This project has received funding from the Innovative Medicines Initiative 2 Joint Undertaking (JU) under grant agreement No 875510 (MM, EJH, EW, IA, ASJ, AK, SKn, FO, KZ, NDE) The JU receives support from the European Union's Horizon 2020 research and innovation programme and EFPIA and Ontario Institute for Cancer Research, Royal Institution for the Advancement of Learning McGill University, Kungliga Tekniska Högskolan, Diamond Light Source Limited. This communication reflects the views of the authors and the JU is not liable for any use that may be made of the information contained herein.

CONFLICT OF INTEREST

OW and TH are listed as inventors on a U.S. patent no. WO2019166639 A1, covering OGG1 inhibitors. The patent is fully owned by a non-profit public foundation, the Helleday Foundation, and TH is a member of the foundation board. MS is an employee of Oxcia, a company developing OGG1 inhibitors. EW, OW, EJH, IA, ASJ, TH and MS are shareholders of Oxcia. The remaining authors declare no competing financial interests.

REFERENCES

[1] S. Oka, J. Leon, K. Sakumi, N. Abolhassani, Z. Sheng, D. Tsuchimoto, F. M. LaFerla, Y. Nakabeppu, *Scientific Reports* **2021**, *11*, 5819.

[2] J. Fukae, M. Takanashi, S. Kubo, K. Nishioka, Y. Nakabeppu, H. Mori, Y. Mizuno, N. Hattori, *Acta Neuropathol.* **2005**, *109*, 256–262.
[3] S. S. B. Komakula, J. Tumova, D. Kumaraswamy, N. Burchat, V. Vartanian, H. Ye, A. Dobrzyn, R. S. Lloyd, H. Sampath, *Sci Rep* **2018**, *8*, 14886.
[4] H. Sampath, V. Vartanian, M. R. Rollins, K. Sakumi, Y. Nakabeppu, R. S. Lloyd, *PLOS ONE* **2012**, *7*, e51697.
[5] J. M. Baquero, C. Benítez-Buelga, V. Rajagopal, Z. Zhenjun, R. Torres-Ruiz, S. Müller, B. M. F. Hanna, O. Loseva, O. Wallner, M. Michel, S. Rodríguez-Perales, H. Gad, T. Visnes, T. Helleday, J. Benítez, A. Osorio, *Scientific Reports* **2021**, *11*, 3490.
[6] T. Visnes, C. Benítez-Buelga, A. Cázares-Körner, K. Sanjiv, B. M. F. Hanna, O. Mortusewicz, V. Rajagopal, J. J. Albers, D. W. Hagey, T. Bekkhus, S. Eshtad, J. M. Baquero, G. Masuyer, O. Wallner, S. Müller, T. Pham, C. Göktürk, A. Rasti, S. Suman, R. Torres-Ruiz, A. Sarno, E. Wiita, E. J. Homan, S. Karsten, K. Marimuthu, M. Michel, T. Koolmeister, M. Scobie, O. Loseva, I. Almlöf, J. E. Unterlass, A. Pettke, J. Boström, M. Pandey, H. Gad, P. Herr, A.-S. Jemth, S. El Andaloussi, C. Kalderén, S. Rodriguez-Perales, J. Benítez, H. E. Krokan, M. Altun, P. Stenmark, U. W. Berglund, T. Helleday, *Nucleic Acids Research* **2020**, *48*, 12234–12251.
[7] M. Hussain, X. Chu, B. Duan Sahbaz, S. Gray, K. Pekhale, J.-H. Park, D. L. Croteau, V. A. Bohr, *Free Radic Biol Med* **2023**, *203*, 34–44.
[8] B. A. Baptiste, S. R. Katchur, E. M. Fivenson, D. L. Croteau, W. L. Rumsey, V. A. Bohr, *Free Radical Biology and Medicine* **2018**, *124*, 149–162.
[9] G. Tian, S. R. Katchur, Y. Jiang, J. Briand, M. Schaber, C. Kreatsoulas, B. Schwartz, S. Thrall, A. M. Davis, S. Duvall, B. A. Kaufman, W. L. Rumsey, *Sci Rep* **2022**, *12*, 14685.
[10] M. Michel, C. Benítez-Buelga, P. A. Calvo, B. M. F. Hanna, O. Mortusewicz, G. Masuyer, J. Davies, O. Wallner, K. Sanjiv, J. J. Albers, S. Castañeda-Zegarra, A.-S. Jemth, T. Visnes, A. Sastre-Perona, A. N. Danda, E. J. Homan, K. Marimuthu, Z. Zhenjun, C. N. Chi, A. Sarno, E. Wiita, C. von Nicolai, A. J. Komor, V. Rajagopal, S. Müller, E. C. Hank, M. Varga, E. R. Scaletti, M. Pandey, S. Karsten, H. Haslene-Hox, S. Loevenich, P. Marttila, A. Rasti, K. Mamonov, F. Ortis, F. Schömberg, O. Loseva, J. Stewart, N. D'Arcy-Evans, T. Koolmeister, M. Henriksson, D. Michel, A. de Ory, L. Acero, O. Calvete, M. Scobie, C. Hertweck, I. Vilotijevic, C. Kalderén, A. Osorio, R. Perona, A. Stolz, P. Stenmark, U. W. Berglund, M. de Vega, T. Helleday, *Science* **2022**, *376*, 1471–1476.
[11] J. C. Fromme, S. D. Bruner, W. Yang, M. Karplus, G. L. Verdine, *Nat Struct Mol Biol* **2003**, *10*, 204–211.
[12] T. Visnes, M. Grube, B. M. Fekry Hanna, C. Benitez-Buelga, A. Cázares-Körner, T. Helleday, *DNA Repair* **2018**, DOI 10.1016/j.dnarep.2018.08.015.
[13] O. Wallner, A. Cázares-Körner, E. R. Scaletti, G. Masuyer, T. Bekkhus, T. Visnes, K. Mamonov, F. Ortis, T. Lundbäck, M. Volkova, T. Koolmeister, E. Wiita, O. Loseva, M. Pandey, E. Homan, C. Benítez-Buelga, J. Davies, M. Scobie, U. W. Berglund, C. Kalderén, P. Stenmark, T. Helleday, M. Michel, *ChemMedChem* **n.d.**, *n/a*, DOI 10.1002/cmdc.202200310.
[14] B. Baños, J. M. Lázaro, L. Villar, M. Salas, M. de Vega, *Nucleic Acids Res* **2008**, *36*, 5736–5749.
[15] S. D. Bruner, D. P. Norman, G. L. Verdine, *Nature* **2000**, *403*, 859–866.
[16] M. Michel, T. Visnes, E. J. Homan, B. Seashore-Ludlow, M. Hedenström, E. Wiita, K. Vallin, C. B. J. Paulin, J. Zhang, O. Wallner, M. Scobie, A. Schmidt, A. Jenmalm-Jensen, U. Warpman Berglund, T. Helleday, *ACS Omega* **2019**, *4*, 11642–11656.
[17] M. Michel, E. J. Homan, E. Wiita, K. Pedersen, I. Almlöf, A.-L. Gustavsson, T. Lundbäck, T. Helleday, U. Warpman Berglund, *Front. Chem.* **2020**, *8*, DOI 10.3389/fchem.2020.00443.
[18] J. Carreras-Puigvert, M. Zitnik, A.-S. Jemth, M. Carter, J. E. Unterlass, B. Hallström, O. Loseva, Z. Karem, J. M. Calderón-Montaño, C. Lindskog, P.-H. Edqvist, D. J. Matuszewski, H. A. Blal, R. P.

A. Berntsson, M. Häggblad, U. Martens, M. Studham, B. Lundgren, C. Wählby, E. L. L. Sonnhammer, E. Lundberg, P. Stenmark, B. Zupan, T. Helleday, *Nature Communications* **2017**, *8*, 1541.
[19] O. Fedorov, F. H. Niesen, S. Knapp, *Methods Mol Biol* **2012**, *795*, 109–118.
[20] H. Gad, T. Koolmeister, A.-S. Jemth, S. Eshtad, S. A. Jacques, C. E. Ström, L. M. Svensson, N. Schultz, T. Lundbäck, B. O. Einarsdottir, A. Saleh, C. Göktürk, P. Baranczewski, R. Svensson, R. P.-A. Berntsson, R. Gustafsson, K. Strömberg, K. Sanjiv, M.-C. Jacques-Cordonnier, M. Desroses, A.-L. Gustavsson, R. Olofsson, F. Johansson, E. J. Homan, O. Loseva, L. Bräutigam, L. Johansson, A. Höglund, A. Hagenkort, T. Pham, M. Altun, F. Z. Gaugaz, S. Vikingsson, B. Evers, M. Henriksson, K. S. A. Vallin, O. A. Wallner, L. G. J. Hammarström, E. Wiita, I. Almlöf, C. Kalderén, H. Axelsson, T. Djureinovic, J. C. Puigvert, M. Häggblad, F. Jeppsson, U. Martens, C. Lundin, B. Lundgren, I. Granelli, A. J. Jensen, P. Artursson, J. A. Nilsson, P. Stenmark, M. Scobie, U. W. Berglund, T. Helleday, *Nature* **2014**, *508*, 215–221.
[21] K. V. M. Huber, E. Salah, B. Radic, M. Gridling, J. M. Elkins, A. Stukalov, A.-S. Jemth, C. Göktürk, K. Sanjiv, K. Strömberg, T. Pham, U. W. Berglund, J. Colinge, K. L. Bennett, J. I. Loizou, T. Helleday, S. Knapp, G. Superti-Furga, *Nature* **2014**, *508*, 222–227.
[22] K. Kubo, H. Ide, S. S. Wallace, Y. W. Kow, *Biochemistry* **1992**, *31*, 3703–3708.
[23] T. Visnes, A. Cázares-Körner, W. Hao, O. Wallner, G. Masuyer, O. Loseva, O. Mortusewicz, E. Wiita, A. Sarno, A. Manoilov, J. Astorga-Wells, A.-S. Jemth, L. Pan, K. Sanjiv, S. Karsten, C. Gokturk, M. Grube, E. J. Homan, B. M. F. Hanna, C. B. J. Paulin, T. Pham, A. Rasti, U. W. Berglund, C. von Nicolai, C. Benitez-Buelga, T. Koolmeister, D. Ivanic, P. Iliev, M. Scobie, H. E. Krokan, P. Baranczewski, P. Artursson, M. Altun, A. J. Jensen, C. Kalderén, X. Ba, R. A. Zubarev, P. Stenmark, I. Boldogh, T. Helleday, *Science* **2018**, *362*, 834–839.